Two tumor specimens per group were processed for immunohistochemical analysis.

Immunohistochemical analysis. Immunohistochemistry was performed on formalin-fixed, paraffin-embedded tissue sections as reported previously.[1,5] An anti-Ki67 monoclonal antibody (clone MIB1; DBA, Milan, Italy) was used and the proportion of positive (proliferating) cells was assessed. At least 1000 cancer cells were counted and scored per slide. Both the percentage of specifically stained cells and the intensity of immunostaining were recorded. Blood vessels were detected with an anti-von Willebrand Factor (vWF) antibody (Chemicon). Microvessel density was determined by calculating the proportion of vWF-positive cells.

Evaluation of apoptosis (TUNEL). Sections were stained with an *in situ* Death Detection POD Kit (Roche Diagnostic GmbH, Mannheim, Germany) according to the manufacturer's instructions. At least 1000 tumor cell nuclei from the most evenly and distinctly labeled areas were examined. The TUNEL-positive tumor cell nuclei were counted, and the apoptotic index was calculated as the proportion of cells with apoptotic nuclei.

Immunoprecipitation and immunoblotting. Cells were maintained in medium without serum for 12 h. Then serum-starved cells were exposed to ZD6474 or gefitinib, incubated for 1 h and stimulated in medium including 10% fetal bovine serum for 30 min. The cells were subsequently washed twice with ice-cold PBS, scraped in lysis buffer (50 m*M* Tris-HCl [pH 8.0], 120 m*M* NaCl, 0.5% Nonidet P-40, 100 m*M* NaF, 200 μ*M* Na_3VO_4, and 10 μg/ml each of aprotinin, leupeptin, and PMSF), and incubated on ice for 60 min. The lysates were centrifuged at 8000*g* for 20 min, and total protein was obtained from the supernatants. Protein concentration was measured with the bicinchoninic acid protein assay (Pierce, Rockford, IL). Cell lysates for immunoprecipitates contained 2 mg of total protein. Anti-EGFR antibody (3 μg) was incubated overnight with the lysates at 4°C, and the precipitates were collected with 40 μliters of Protein G Sepharose beads over a 1 h period. Antibody-complexed proteins were washed with lysis buffer, analyzed by SDS-PAGE and visualized using an enhanced chemiluminescence solution (ECL; Amersham Pharmacia Biotech UK, Buckinghamshire, UK). Quantative analysis was performed using Kodak software. Quantified values of phospho-EGFR bands were standardized according to those of EGFR bands.

Results

***In vitro* evaluation of ZD6474 and gefitinib inhibition of tumor cell growth.** The IC_{50} values of gefitinib for growth inhibition of PC-9 and PC-9/ZD cells were 0.038 μ*M* and 6.8 μ*M*, respectively. The IC_{50} values of ZD6474 were 0.14 μ*M* and 5.92 μ*M*, respectively (Fig. 1A). PC-9 cells were 180-fold more sensitive to gefitinib than PC-9/ZD cells, and PC-9/ZD cells were cross-resistant to ZD6474. Experiments with another VEGFR-TKI, SU5416, and PDGFR-TKI, Tyrphostin 9, revealed no cross-resistance (data not shown).

In a separate experiment, the IC_{50} values of gefitinib were 0.006 μ*M* and 20.5 μ*M*, in PC-9 and PC-14 (another human NSCLC cell line), respectively (Fig. 1B). PC-9 cells were therefore approximately 3400-fold more sensitive to gefitinib than PC-14 cells. Corresponding IC_{50} values for ZD6474 were 0.11 μ*M* and 9.81 μ*M*, demonstrating cross-resistance to ZD6474.

Other workers have examined the ability of gefitinib or ZD6474 to inhibit serum-dependent tumor cell growth *in vitro*, and have demonstrated IC_{50} values of gefitinib[12] and ZD6474[13] of >1 μ*M* for tumor cell lines. Therefore, PC-9 is particularly sensitive to *in vitro* growth inhibition by both gefitinib and ZD6474, whereas the sensitivities of both gefitinib-resistant PC-9/ZD and PC-14 fall within the normal range reported for other tumor cell lines.

***In vivo* antitumor effects.** ZD6474 treatment (12.5–50 mg/kg/day) resulted in inhibition of PC-9 tumor growth, with robust tumor regression seen even at the lowest dose tested. ZD6474 treatment also resulted in dose-dependent inhibition of PC-9/ZD tumor xenograft growth, although in this case, regression was not seen (Fig. 2, A and B). This antitumor effect of ZD6474 was very similarly to that of gefitinib we previously reported (Fig. 2, C and D).[8]

Effect of treatment on cell proliferation, apoptosis, and vascularization. ZD6474 treatment resulted in a dose-dependent decrease in the proportion of proliferating cells in the PC-9 tumors, but not in PC-9/ZD xenografts (Fig. 3). No significant

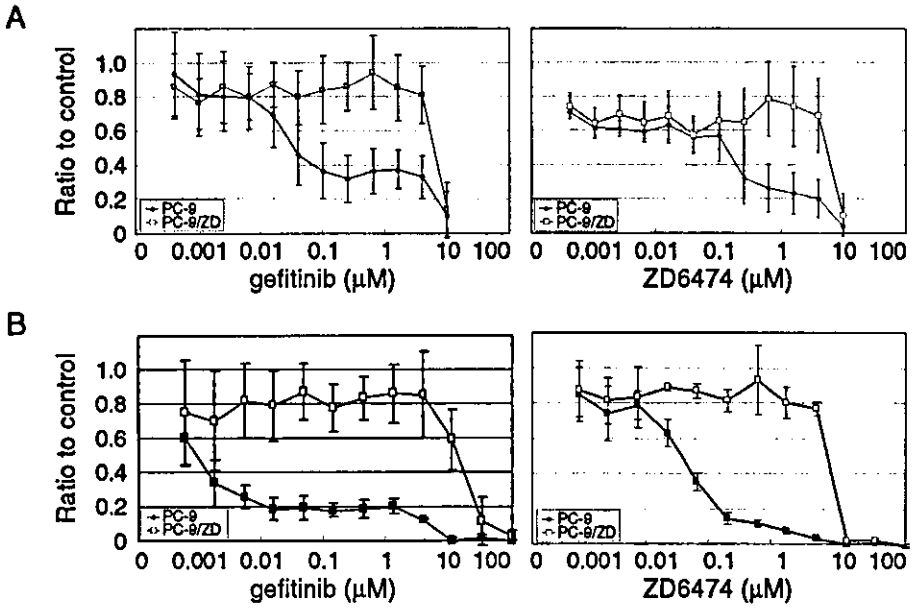

Fig. 1. Growth inhibitory effect of gefitinib (ZD1839) and ZD6474. A: PC-9 and PC-9/ZD, B: PC-9 and PC-14 cells. Data shown are mean values from three experiments (±SD).

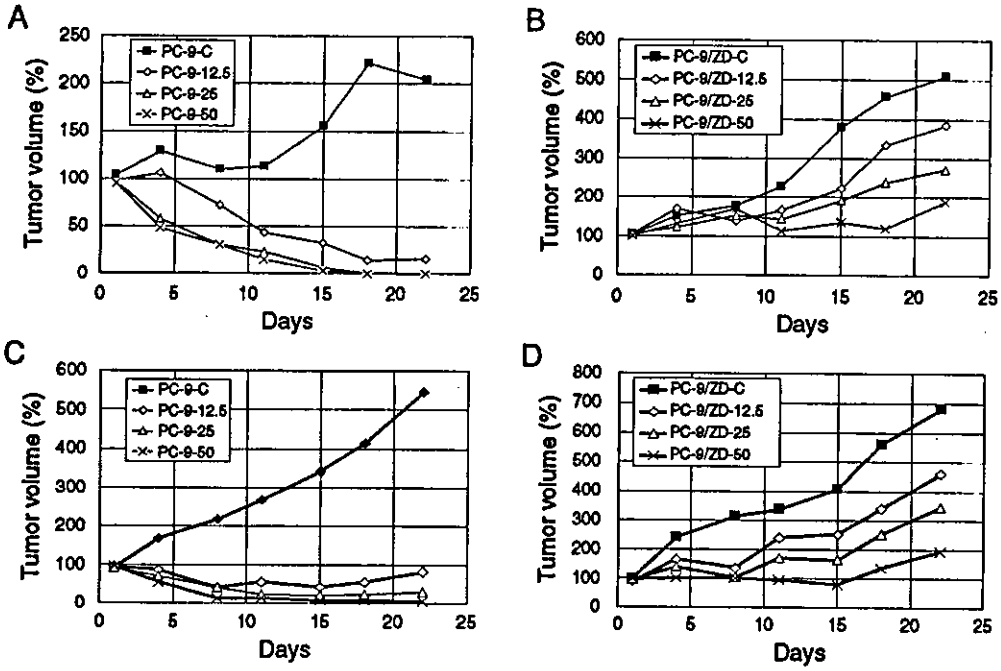

Fig. 2. Antitumor activity of ZD6474 (A, B) and gefitinib (C, D) on established PC-9 (A, C) and PC-9/ZD (B, D) human lung cancer xenografts.

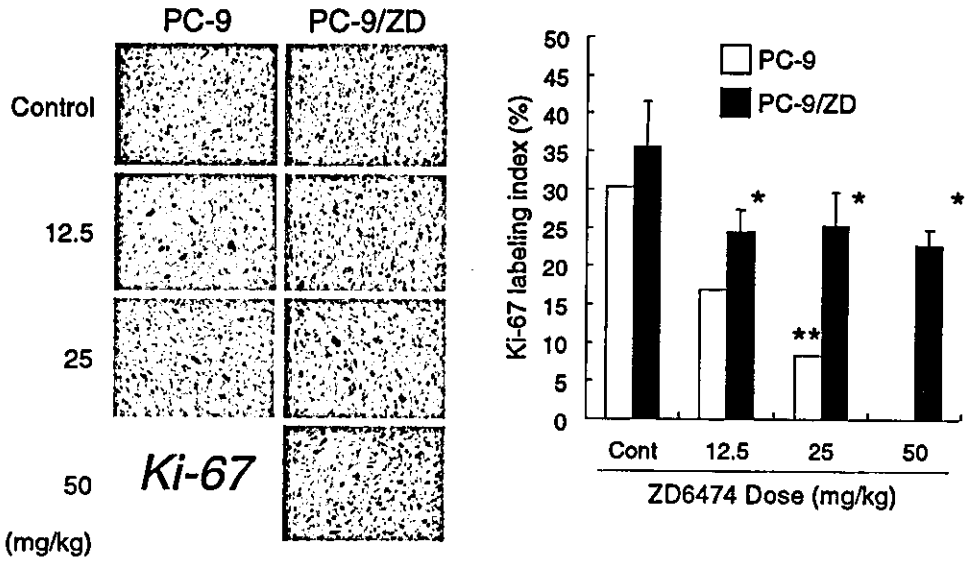

Fig. 3. Effect of ZD6474 on the Ki67 labeling index of PC-9 and PC-9/ZD tumors *in vivo*. Data represent mean values (±SD). Significant difference from control shown by the Dunnett test (* $P<0.05$, ** $P<0.01$).

increase in apoptosis was observed in either tumor type (Fig. 4).

Assessment of tumor vascularization showed a significant reduction in vascular density following ZD6474 treatment of PC-9 tumor xenografts, although no effect was seen in PC-9/ZD tumors (Fig. 5). Differences in the action of ZD6474 on PC-9 and PC-9/ZD tumors are summarized in Table 1.

Inhibition of EGFR activity. It is possible that the antitumor activity of ZD6474 is partly attributable to EGFR inhibition based on the evidence of cross-resistance to gefitinib (Figs. 1–3). Therefore, site-specific anti-phosphorylated-EGFR antibodies were used to investigate inhibition of EGFR phosphorylation by ZD6474 in PC-9 and PC-9/ZD cells at four different tyrosine phosphorylation sites (Tyr845, Tyr992, Tyr1045, and Tyr1068; Fig. 6). ZD6474 dose-dependently inhibited phosphorylation of the four EGFR tyrosine residues in PC-9 cells (Fig. 6). In PC-9/ZD cells, drug-related inhibition of phosphorylation at the Tyr992 site was highly resistant to ZD6474 treatment (Fig. 6), and the Tyr845 and Tyr1045 sites were moderately resistant, while the effect of phosphorylation at the Tyr1068 site did not differ significantly between the sensitive and resistant cell lines (Table 1). The spectrum of activity of ZD6474 on the

four EGFR tyrosine residues examined in PC-9/ZD cells differed from that of gefitinib. ZD6474 displayed a variety of actions on each tyrosine residue, which may be responsible for the wide range of biological activities.

Discussion

In the NSCLC xenograft model reported here, ZD6474 treatment significantly inhibited PC-9 tumor growth, inducing tumor regression. In addition, ZD6474 caused dose-dependent PC-9/ZD tumor growth inhibition. These data indicate that ZD6474 exerts potent antitumor activity against gefitinib-sensitive and resistant lung cancers *in vivo*. Although PC-9/ZD cells are less sensitive to gefitinib than PC-9 cells, the *in vitro* sensitivity of these cells falls within the normal range for other tumor cell lines. Accordingly, gefitinib has significant *in vivo* activity against PC-9/ZD, producing a dose-dependent inhibition of xenograft growth, rather than the tumor regression seen with PC-9 xenografts. Therefore, the antitumor activity of ZD6474 appeared to parallel that of gefitinib in PC-9 and PC-9/ZD tumor cells, both *in vitro* and *in vivo*. Since gefitinib is a TKI with a high degree of selectivity for EGFR,[1,2,4] inhibition of EGFR autophosphorylation is likely to contribute to the antitumor activity of ZD6474, particularly in tumor cells which are dependent on EGFR signaling for continued growth and survival. This was shown *in vitro*, as ZD6474 inhibited EGFR

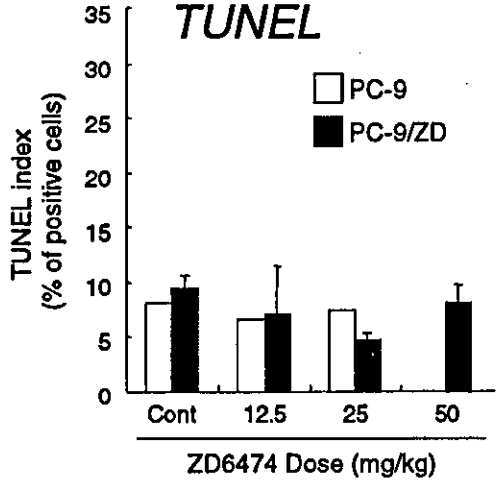

Fig. 4. Effect of ZD6474 on the TUNEL index of PC-9 or PC-9/ZD tumors *in vivo*. Data represent mean values (±SD).

Table 1. Site-specific effect of ZD6474 on EGFR tyrosine residues in PC-9 and PC-9/ZD cells

Tyr residue of EGFR	Inhibition of phosphorylation			
	ZD6474		Gefitinib	
	PC-9	PC-9/ZD	PC-9	PC-9/ZD
845	++	+	++	+
992	++	–	++	++
1045	++	+	–	–
1068	++	++	++	+

++ strong; + moderate; – not significant.

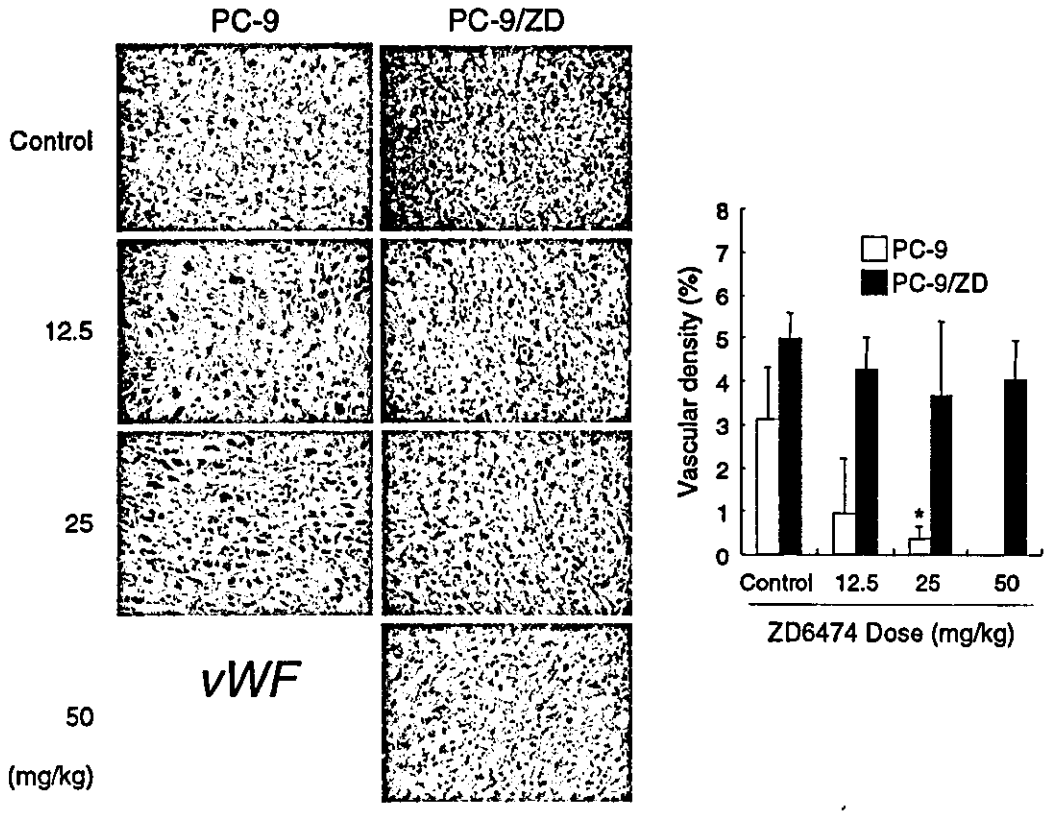

Fig. 5. Effect of ZD6474 on the vascular density of PC-9 and PC-9/ZD tumors stained *in vivo* with anti-vWF. Values are means±SD. Significant difference from the control by the Dunnett test (* $P<0.05$).

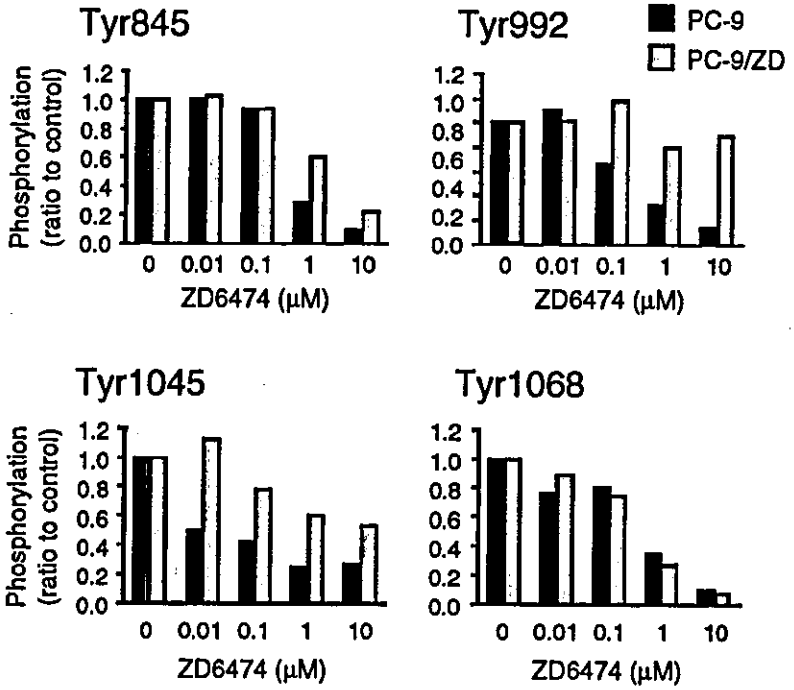

Fig. 6. Phosphorylation of EGFR tyrosine residues in PC-9 and PC-9/ZD cells after exposure to ZD6474.

phosphorylation in a dose-dependent manner. These results are consistent with previous reports[1] and indicate that ZD6474 is a potent EGFR TKI. *In vivo*, ZD6474 decreased vascular density in PC-9 tumors but not in PC-9/ZD cells, suggesting that ZD6474 may affect the angiogenic process via EGFR blockade. This could be mediated by inhibition of EGFR-induced paracrine production of angiogenic growth factors, such as VEGF, bFGF, and TGF from cancer cells, but the exact mechanism of action is unclear. This activity is, however, likely to be of less significance than the VEGFR-2-mediated antiangiogenic effect, since ZD6474 has been shown to have consistent *in vivo* antitumor activity in a range of histologically diverse human tumor xenografts, including activity in tumor models which do not respond to treatment with an EGFR TKI.[13] In addition, any change, or lack of change in microvessel density needs to be interpreted with caution as a either positive or negative indication of antiangiogenic activity, since the efficacy of antiangiogenic agents may not be related to microvessel density measurements.[14] ZD6474 was expected to induce increased apoptosis in tumor cells; although no induction of apoptosis was in fact observed, this may have been due to experimental factors.

Phosphorylations of Tyr845 and Tyr1045 of PC-9 and PC-9/ZD cells are similarly inhibited by ZD6474. On the other hand, while the inhibition pattern of Tyr845 phosphorylation by ZD6474 is coincident with that by gefitinib, the patterns at Tyr1045 are different. Therefore, we considered that the Tyr1045 is more important than Tyr845 for assessing the distinctive mode of action of ZD6474. In searching for a common mode of action of ZD6474 and gefitinib, Tyr845 seems to be the most promising site.

Phosphorylation of Tyr992 has been reported to transduce the signal to phospholipase C and protein kinase C.[15–17] In contrast, no inhibition of pan-phospho-PKC (the downstream signal of Tyr992) by gefitinib or ZD6474 was observed (data not shown). Tyr1045 has been reported to be linked to the Cbl-ubiquitin signaling pathway.[18] We have previously reported that Tyr1068 is a possible target site of EGFR for gefitinib[7], and gefitinib inhibited phosphorylation of Tyr1068 to varying degrees in PC-9 and PC-9/ZD cells, whereas ZD6474 inhibited Tyr1068 in both cell lines. These results suggest that the mode of inhibition of phosphorylation of EGFR by ZD6474 is subtly different to that of gefitinib. Therefore, although ZD6474 shows cross-resistance to gefitinib in these PC-9/ZD tumor cells, it has the potential for activity against gefitinib-resistant tumors through at least two mechanisms: (i) inhibition of EGFR-dependent downstream signaling pathways through differential effects on the phosphorylation status of tyrosine residues in the intracellular domain of EGFR, and (ii) inhibition of tumor angiogenesis through inhibition of VEGFR2 tyrosine kinase activity, which has not been examined in the present study. Site-directed mutagenesis studies are now under way to elucidate the biological significance of these sites.

1. Ciardiello F, Caputo R, Damiano V, Troiani T, Vitagliano D, Carlomagno F, Veneziani BM, Fontanini G, Bianco AR, Tortora G. Antitumor effects of ZD6474, a small molecule vascular endothelial growth factor receptor tyrosine kinase inhibitor, with additional activity against epidermal growth factor receptor tyrosine kinase. *Clin Cancer Res* 2003; 9: 1546–56.
2. Ciardiello F, Bianco R, Caputo R, Damiano V, Troiani T, Melisi D, De Vita F, De Placido S, Bianco AR, Tortora G. Antitumor activity of ZD6474, a vascular endothelial growth factor receptor tyrosine kinase inhibitor, in human cancer cells with acquired resistance to antiepidermal growth factor receptor therapy. *Clin Cancer Res* 2004; 10: 784–93.
3. Minami H, Ebi H, Tahara M, Sasaki Y, Yamamoto N, Yamada Y, Tamura T, Saijo N. A phase I study of an oral VEGF receptor tyrosine kinase inhibitor ZD6474, in Japanese patients with solid tumors. *Proc Am Soc Clin Oncol* 2003; 22: abstr 778.
4. Hurwitz H, Holden SN, Eckhardt SG, Rosenthal M, de Boer R, Rischin D, Green M, Basser R. Clinical evaluation of ZD6474, an orally active inhibitor of VEGF signaling, in patients with solid tumors. *Proc Am Soc Clin Oncol* 2002; 22: abstr 325.
5. Ciardiello F, Caputo R, Bianco R, Damiano V, Pomatico G, De Placido S, Bianco AR, Tortora G. Antitumor effect and potentiation of cytotoxic drugs activity in human cancer cells by ZD-1839 (Iressa), an epidermal growth factor receptor-selective tyrosine kinase inhibitor. *Clin Cancer Res* 2000; 6: 2053–63.
6. Moasser MM, Basso A, Averbuch SD, Rosen N. The tyrosine kinase inhibi-

tor ZD1839 ("Iressa") inhibits HER2-driven signaling and suppresses the growth of HER2-overexpressing tumor cells. *Cancer Res* 2001; 61: 7184–8.
7. Koizumi F, Kanzawa F, Ueda Y, Koh Y, Tsukiyama S, Taguchi F, Tamura T, Saijo N, Nishio K. Synergistic interaction between the EGFR tyrosine kinase inhibitor gefitinib ("Iressa") and the DNA topoisomerase I inhibitor CPT-11 (irinotecan) in human colorectal cancer cells. *Int J Cancer* 2004; 108: 464–72.
8. Koizumi F, Taguchi F, Shimoyama T, Saijo N, Nishio K. Mechanism of resistance to epidermal growth factor receptor inhibitor ZD1839: a role for inhibiting phosphorylation of EGFR at Tyr1068. *Am Assoc Cancer Res* 2003: abstr 1001.
9. Kawamura-Akiyama Y, Kusaba H, Kanzawa F, Tamura T, Saijo N, Nishio K, Arioka H, Ishida T, Fukumoto H, Kurokawa H, Sata M, Ohata M, Morikage T, Ohmori T, Fujiwara Y, Takeda Y. Non-cross resistance of ZD0473 in acquired cisplatin-resistant lung cancer cell lines. *Lung Cancer* 2002; 38: 43–50.
10. Nishio K, Arioka H, Ishida T, Fukumoto H, Kurokawa H, Sata M, Ohata M, Saijo N, Morikage T, Ohmori T, Fujiwara Y, Takeda Y. Enhanced interaction between tubulin and microtubule-associated protein 2 via inhibition of MAP kinase and CDC2 kinase by paclitaxel. *Int J Cancer* 1995; 63: 688–93.
11. Naruse I, Ohmori T, Ao Y, Fukumoto H, Kuroki T, Mori M, Saijo N, Nishio K. Antitumor activity of the selective epidermal growth factor receptor-tyrosine kinase inhibitor (EGFR-TKI) Iressa (ZD1839) in an EGFR-expressing multidrug-resistant cell line *in vitro* and *in vivo*. *Int J Cancer* 2002; 98: 310–5.
12. Ono M, Hirata A, Kometani T, Miyagawa M, Ueda S, Kinoshita H, Fujii T, Kuwano M. Sensitivity to gefitinib (Iressa, ZD1839) in non-small cell lung cancer cell lines correlates with dependence on the epidermal growth factor (EGF) receptor/extracellular signal-regulated kinase 1/2 and EGF receptor/Akt pathway for proliferation. *Mol Cancer Ther* 2004; 3: 465–72.
13. Wedge SR, Ogilvie DJ, Dukes M, Kendrew J, Chester R, Jackson JA, Boffey SJ, Valentine PJ, Curwen JO, Musgrove HL, Graham GA, Hughes GD, Thomas AP, Stokes ES, Curry B, Richmond GH, Wadsworth PF, Bigley AL, Hennequin LF. ZD6474 inhibits vascular endothelial growth factor signaling, angiogenesis, and tumor growth following oral administration. *Cancer Res* 2002; 62: 4645–55.
14. Hlatky L, Hahnfeldt P, Folkman J. Clinical application of antiangiogenic therapy: microvessel density, what it does and doesn't tell us. *J Natl Cancer Inst* 2002; 94: 883–93.
15. Holbrook MR, O'Donnell JB Jr, Slakey LL, Gross DJ, Bishayee A, Beguinot L, Bishayee S. Epidermal growth factor receptor internalization rate is regulated by negative charges near the SH2 binding site Tyr992. *Biochemistry* 1999; 38: 9348–56.
16. Bishayee A, Beguinot L, Bishayee S. Phosphorylation of tyrosine 992, 1068, and 1086 is required for conformational change of the human epidermal growth factor receptor c-terminal tail. *Mol Biol Cell* 1999; 10: 525–36.
17. Nogami M, Yamazaki M, Watanabe H, Okabayashi Y, Kido Y, Kasuga M, Sasaki T, Maehama T, Kanaho Y, Holbrook MR, O'Donnell JB Jr, Slakey LL, Gross DJ, Bishayee A, Beguinot L, Bishayee S. Requirement of autophosphorylated tyrosine 992 of EGF receptor and its docking protein phospholipase C gamma 1 for membrane ruffle formation. *FEBS Lett* 2003; 536: 71–6.
18. Ravid T, Sweeney C, Gee P, Carraway KL 3rd, Goldkorn T. Epidermal growth factor receptor activation under oxidative stress fails to promote c-Cbl mediated down-regulation. *J Biol Chem* 2002; 277: 31214–9.

Synergistic interaction between gefitinib (Iressa, ZD1839) and paclitaxel against human gastric carcinoma cells

Jong-Kook Park[a], Sang-Hak Lee[a], Jin-Hyoung Kang[b], Kazuto Nishio[c], Nagahiro Saijo[c] and Hyo-Jeong Kuh[a]

We have evaluated the antitumor effects of gefitinib (Iressa, ZD1839) in SNU-1 human gastric cancer cells (hMLH1-deficient and epidermal growth factor receptor-overexpressed) when given alone or as a doublet with oxaliplatin (LOHP), 5-fluorouracil (5-FU) or paclitaxel (PTX). The four drugs showed IC_{50}s ranging from 1.81 nM to 13.2 μM. LOHP and PTX induced G_2/M arrest, 5-FU increased S phase, and gefitinib increased G_1 in a concentration-dependent manner. The analysis using the previously developed cytostatic TP_i model showed that 64 and 80% of the overall growth inhibition was attributed to cell cycle arrest in cells exposed to 7.55 μM of LOHP or 10 nM of PTX for 72 h, respectively. PTX + gefitinib showed greatest synergism as determined by combination index analysis and apoptosis induced by PTX was potentiated by the co-administration of gefitinib. LOHP + gefitinib showed a similar, although to a lesser degree, synergistic effect. This study demonstrates the antitumor activity and the significant cell cycle arrest induced by gefitinib in SNU-1 human gastric carcinoma cells, and its synergistic interaction with LOHP and PTX. *Anti-Cancer Drugs* **15:809–818 © 2004 Lippincott Williams & Wilkins.**

Anti-Cancer Drugs 2004, 15:809–818

Keywords: combination, gefitinib (ZD1839), human gastric carcinoma, oxaliplatin, paclitaxel

[a]Research Institute of New Drug Development, Catholic Research Institutes of Medical Science and [b]Division of Medical Oncology, The Catholic University of Korea, Seoul, South Korea and [c]Support Facility of Project Ward, National Cancer Center Hospital, Tokyo, Japan

Sponsorship: This work was supported in part by a grant from the Korea Health 21 R&D Project, Ministry of Health & Welfare (02-PJ2-PG1-CH12-0002), and by a grant from KOSEF (R04-2000-000-00052-0), Republic of Korea.

Correspondence to H.-J. Kuh, Catholic Research Institutes of Medical Science, Catholic University of Korea, 505 Banpo-dong, Seocho-ku, Seoul 137-401, South Korea.
Tel: +82 2 590 2422; fax: +82 2 592 2421;
e-mail: hkuh@catholic.ac.kr

Received 23 February 2004 Revised form accepted 4 June 2004

Introduction

The contemporary combination regimens for treatment of gastric cancer usually contain cisplatin and 5-fluorouracil (5-FU). Recently, the triplet combination of cisplatin, 5-FU and paclitaxel (PTX) has become one of the most highly active regimens against advanced gastric carcinoma [1].

Tumor tissues from gastric cancer patients show a high incidence of epidermal growth factor (EGF) and its receptor (EGFR) overexpression, both of which play a promotional role in the development of gastric cancer cooperatively with other members of the EGFR gene family, c-erbB-2 and c-erbB-3 [2]. The EGF and EGFR gene families have been associated with the growth regulation and gastric wall invasion in gastric cancers [3,4], and seem to be involved in determining the chemosensitivity of human cancer cells to chemotherapy [5]. Recently, it was also reported that inhibition of the EGFR cascade abrogated *Helicobacter pyroli*-induced up-regulation of vascular endothelial growth factor in gastric cancer cells [6]. A novel approach for the therapeutic blockade of EGFR signaling in human cancer has been recently developed based on the discovery of low-molecular-weight compounds that selectively inhibit the ligand-induced activation of EGFR tyrosine kinase (TK) and its receptor-mediated intracellular signaling [7]. Among various quinazoline-derived compounds tested as new anticancer drugs, gefitinib ([4-(3-chloro-4-fluoroanilino)-7-methoxy-6-(3-morpholinopropoxy) quinazoline], also 'Iressa', ZD1839) has shown impressive preclinical activity in various tumor models *in vitro* and *in vivo* [7]. It is an orally active, selective EGFR-TK inhibitor that blocks the signal transduction pathways implicated in the proliferation and survival of cancer cells, and is currently under phase III clinical trial [7,8].

In addition, the methylation of DNA mismatch repair (MMR) genes has been observed in many human cancers, including gastric cancers. The methylation of the hMLH-1 promoter region has been shown to be involved in the mechanism of low or undetectable hMLH-1 protein expression in gastric tumors [9,10]. In addition to predisposing oncogenesis, the loss of MMR activity is related to drug resistance, since the MMR proteins play important roles in mediating the activation of cell cycle checkpoints and apoptosis in response to DNA damage induced by anticancer agents. This drug resistance extends to a variety of alkylating anticancer agents including platinum compounds, such as cisplatin and carboplatin [11]. Moreover, it has been shown that *N*-methyl-*N'*-nitro-*N*-nitrosoguanidine (MNNG)-resistant

0959-4973

human gastric cancer cells have very low or undetectable levels of hMLH-1 protein, which plays a key role with hMSH2 in the MMR system [12].

Oxaliplatin (LOHP) has a spectrum of activity that differs from that of cisplatin or carboplatin, suggesting that it has different molecular targets and/or different mechanism of resistance. It has been reported that MMR deficiencies do not induce similar resistance to LOHP [13], and because of this decreased possibility of resistance development, LOHP may serve as a good candidate for first-line treatment as a monotherapy or in combination with other agents in gastric cancer. Hence, LOHP may effectively substitute for cisplatin in the platinum-based triplet combination with 5-FU and PTX, as mentioned above.

In many studies, gefitinib in combination with radiation as well as a variety of cytotoxic agents, including taxanes and platinum compounds, has shown synergistic and supra-additive interactions in many types of cancers, such as colon, lung, breast, prostate and ovarian cancer [14]. However, no studies have been conducted on the antitumor effects of gefitinib given alone or in combination with cytotoxic agents against human gastric cancer cells.

In the present study, we evaluated the growth-inhibitory and cell cycle arrest effects of LOHP, 5-FU and PTX, which are promising cytotoxic drugs for the treatment of gastric carcinoma, and of a target-based cytostatic drug, gefitinib, in SNU-1 human gastric carcinoma cells that show MMR deficiency and EGFR overexpression. We also determined whether simultaneous EGFR blockade by gefitinib could improve the anticancer activities of these cytotoxic drugs. Our results show that the gefitinib + PTX combination had the greatest synergistic interaction. Gefitinib was found to potentiate the apoptosis induced by PTX.

Materials and methods

Chemicals

Clinical grade gefitinib and LOHP were kindly provided by AstraZeneca Pharmaceuticals (Macclesfield, UK) and Sanofi-Synthelabo (Malvern, PA), respectively. PTX and 5-FU were provided by the Drug Synthesis and Chemistry Branch, Developmental Therapeutics Program, Division of Cancer Treatment and Diagnosis, NCI (Bethesda, MD). Other drugs and reagents, unless otherwise stated, were purchased from Sigma (St Louis, MO).

Cell culture conditions

The human gastric cancer cell lines, SNU-1 and MKN-45, human lung adenocarcinoma cell line, A549, and human epidermoid carcinoma cell line, A431 were obtained from the Korean Cell Line Bank (Seoul, South Korea). Cells were maintained in RPMI 1640 supplemented with 10% heat-inactivated fetal bovine serum, 100 mg/ml of streptomycin and 100 U/ml penicillin in humidified air containing 5% (v/v) CO_2 at 37°C.

Western blotting

Total cell protein extracts were obtained as previously described [15]. Briefly, cells were lysed with lysis buffer [20 mM Tris–HCl (pH 7.5), 150 mM NaCl, 0.1% SDS, 1% Triton X-100, 1% sodium deoxycholate]. The lysate, containing 30 μg of total protein, was then mixed with 2 × SDS–PAGE sample buffer, boiled for 5 min and electrophoresed in 8% SDS gels under reducing conditions. The separated proteins were then electrophoretically transferred to PVDF membranes (Millipore, Bedford, MA) and the membranes were probed with a primary antibody against EGFR or hMLH1 (anti-human EGFR rabbit polyclonal antibody and anti-human hMLH1 rabbit polyclonal antibody; Santa Cruz Biotechnology, Santa Cruz, CA) at 1:1000 dilution. Immunoreactive proteins were detected by using an enhanced chemiluminescence detection system (Amersham Pharmacia Biotech, Little Chalfont, UK).

Measurement of growth inhibition

Growth inhibitory effects were measured by MTT assay and by direct cell counting [16]. For MTT assay, cells were plated in 96-well microtiter 24 h prior to treatment (4000 cells/well). Cells were exposed to various concentrations of the tested agents for 72 h. The absorbance of the reaction mixture was measured at 540 nm and the IC_{50} defined as the drug concentration required to reduce the absorbance to 50% of the control in each test was determined using an E_{max} model:

$$\%\ \text{Cell viability} = (100 - R) \times \left(1 - \frac{[D]^m}{K_d^m + [D]^m}\right) + R \quad (1)$$

where D is the drug concentration, K_d is the concentration of the drug that produces a 50% reduction in absorbance (i.e. IC_{50}), m is the Hill-type coefficient and R is the residual unaffected fraction (the resistant fraction). The Sigma Plot regression function was used for model fitting.

For direct cell counting, cells were seeded at a density of 1×10^6 in 100- or 150-mm Petri dishes at least 24 h prior to drug exposure and were exposed to two different concentrations of the drug for up to 72 h. The concentrations of each drug were 0.75 and 7.55 μM for LOHP, 9 and 65 μM for 5-FU, 2.5 and 10 nM for PTX, and 13 and 38 μM for gefitinib. At predetermined times, cells were harvested by resuspending then in PBS and then the total cell number was determined using a Counter (Coulter Electronics, Luton, UK). Trypan blue

exclusion under the microscope was used to determine the viable cell fraction. The remainder of the cell suspension samples was used for the cell cycle study (see below). For the combination study, gefitinib was given simultaneously with either LOHP, 5-FU or PTX for 72 h. Drugs were combined at equitoxic ratios (i.e. doses were applied in combinations that would have produced the same cytotoxic effect if the drugs were administered separately to produce a 50% growth inhibition, as determined by MTT assay). The cytotoxicities of the two-drug combinations were determined by MTT assay using the same procedure as used for single treatments. Each experiment was performed in triplicate.

Determination of combination effects

The cytotoxic effects obtained with two-drug combinations were analyzed using the Chou and Talalay method [17]. The interaction between two drugs was assessed by using combination index (CI) (2). CI was calculated for a cell death range of 20–80 %, i.e. CI_{20}–CI_{80}.

$$CI_x = \frac{(D)_A}{(D_x)_A} + \frac{(D)_B}{(D_x)_B} + \alpha \cdot \frac{(D)_A(D)_B}{(D_x)_A(D_x)_B} \qquad (2)$$

where CI_x is the CI for a fixed effect, x [fraction affected (f_a)·100], for a combination of drug A and drug B, $(D_x)_A$ is the concentration of drug A alone giving an effect x, $(D_x)_B$ is the concentration of drug B alone giving an effect x, $(D)_A$ is the concentration of drug A in combination A + B giving an effect x, $(D)_B$ is the concentration of drug B in combination A + B giving an effect x, and α is a parameter with value 0 when A and B are mutually exclusive and 1 when A and B are mutually non-exclusive. A CI_x between 0.8 and 1.2 was categorized as additive, less than 0.8 as synergistic, and greater than 1.2 as antagonistic.

Measurement of cell cycle effect

Cells were plated and treated as described above (see measurement of growth inhibition by direct cell counting). For the combination of PTX and gefitinib, cells were exposed to 1.25 nM of PTX and 8.5 μM of gefitinib or 0.6 nM of PTX and 4 μM of gefitinib. After harvesting, the cells were fixed in 10 ml of 70% cold ethanol while vortexing, and cells were kept at 4°C for 1 h and stored at –20°C until analysis. Upon analysis, fixed cells were washed and resuspended in 1 ml of PBS containing 50 μg/ml RNase A and 50 μg/ml propidium iodide. After 20 min incubation at 37°C, cells were analyzed for DNA content by flow cytometry (FACSVantage; Becton Dickinson Immunocytometry Systems, San Jose, CA). For each sample, 10 000 events were acquired. Cell cycle distribution was determined using cell cycle analysis software (Modfit; Verity, Topsham, ME).

Cytostatic model analysis

In order to predict the contribution of cell cycle arrest to the overall growth inhibition induced by a cytotoxic agent, we used the cytostatic TP_i model as described previously [18]. In brief, the model assumptions were: (1) exponential growth of a cell population with a growth rate constant (k); (2) all cells were in cycle, i.e. no cell deaths and no G_0 phase arrest; (3) that the distribution of cell numbers in a cell cycle follows the age structure of a simple exponential population. $TP_i(t)$, the transition probability for i phase at time t, was defined as $(\alpha_i(t)-\alpha_i(t+\Delta t))/\alpha_i(t)/\Delta t$, where $\alpha_i(t) = [N_i(t)-(\#$ cells already exiting from i phase at time $t)]/N_i(t)$ and $N_i(t)$ is the number of cells in i phase at time t. The transition probability for each cell cycle check point, i.e. $TP_{G1}(t)$, $TP_S(t)$ and $TP_{G2/M}(t)$, was calculated using $F_i(t)$, the fraction of cells in the G_1, S and G_2/M phases at time t, and $k(t)$, the growth rate constant. The simulation of cell population growth over time was performed using a numerical method based on the cell population growth algorithm using $TP_i(t)$ and $F_i(t)$. This model assumes no cell death during cell cycle progression; hence, the simulation result represents a reduction in the number of cells resulting from cell cycle arrest (or disturbed cell cycle progression) only. The model should underestimate growth inhibition in the presence of cell death and the difference between the model-predicted and the observed growth curve of a treated cell population represents the growth inhibition resulting from cell death in the population.

Simultaneous measurement of drug-induced apoptosis and cell cycle distribution

For simultaneous determination of cell cycle contents and apoptosis, the user's manual of Apo-Direct kit (PharMingen, San Diego, CA) was followed. Briefly, after harvest, cells were fixed in 1% paraformaldehyde/PBS on ice for 15 min and resuspended in 70% ice-cold ethanol. Cells were then incubated in 50 μg of solution containing terminal deoxynucleotidyltransferase and FITC-conjugated dUTP deoxynucleotides 1:1 in reaction buffer for 2 h at 37°C in the dark. After washing in PBS containing 0.1% Triton X-100, the cells were stained with 5 μg of propidium iodide and 10 kU of RNase in 1 ml of PBS for 20 min at 37°C. Flow cytometric analysis was performed with FL1 (FITC) and FL2 (propidium iodide) and data acquisition and analysis were done using CellQuest software (Becton Dickinson Immunocytometry Systems).

Statistical analysis

Statistical comparisons were completed using Student's paired t-test; $p < 0.05$ was considered statistically significant.

Results

hMLH-1 and EGFR expression in SNU-1 and MKN45

We evaluated the antitumor activities of the three cytotoxic drugs, LOHP, 5-FU or PTX, and that of a cytostatic drug, gefitinib, alone and in doublet combinations. We selected SNU-1 human gastric carcinoma cells because they are known to be MMR deficient due to a

missense mutation in hMLH-1 [12], which was confirmed in this study (Fig. 1A). EGFR expression was also examined and significant expression was observed in these cells. The level of expression was higher than those in MKN-45, another human gastric cancer cell line, and in A549, a human lung cancer cell line (Fig. 1B and 1C). Hence, SNU-1 cells were considered to represent an *in vitro* gastric cancer model that may have intrinsic chemoresistance related to both MMR deficiency and EGFR overexpression.

Cytotoxicity of LOHP, 5-FU, PTX and gefitinib in SNU-1 cells

Dose–response curves were analyzed using an E_{max} model with a resistant fraction (R), which represents the fraction of cells insensitive to the drug (Table 1). Significant R values were obtained for PTX (mean of 32%), whereas the other three drugs showed a full dose–response curve with percentage cell viabilities decreasing almost to the base line level (< 10%). The IC_{50} showed a wide range from 1.81 nM to 13.2 μM, i.e. 0.788 μM for LOHP, 9.35 μM for 5-FU, 1.81 nM for PTX and 13.2 μM for gefitinib. The antiproliferative activity of these agents was confirmed by direct cell counting. Drugs were given at two different concentrations, i.e. at the IC_{50} and IC_{80} levels. For all agents, 72 h exposure exhibited 50–60 and 80–90% growth inhibition at the IC_{50} and IC_{80} drug concentrations, respectively (Fig. 2). For PTX, 10 nM induced 68% growth inhibition when measured by MTT assay, with no further inhibition at higher concentrations, nonetheless, 89% inhibition was observed by direct cell counting (Fig. 2C).

Fig. 1

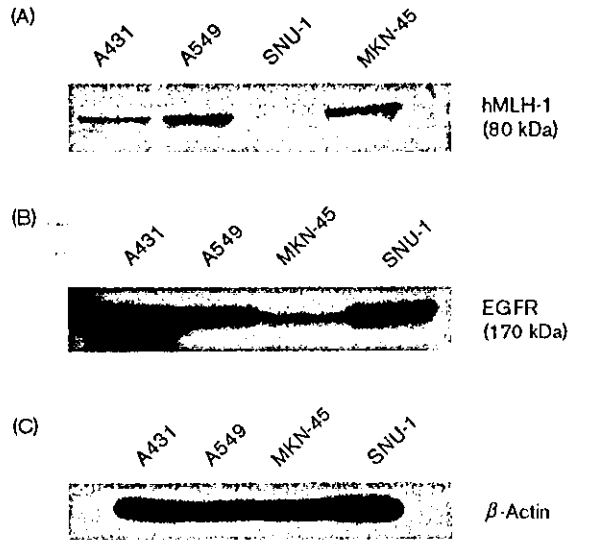

Western blot analysis of hMLH-1 (A) and EGFR (B) expression in A549, A431, SNU-1 and MKN-45 cells. The relative expression levels of EGFR relative to β-actin (C) were compared for these four cell lines.

Cytostatic model analysis

Growth inhibition, i.e. the reduction in the growth rate of a cell population following drug treatment, is the result of cell cycle arrest (cytostatic effect) and cell death (cytotoxic effect). As previously reported, we have developed a computational model (a cytostatic model, because the model assumes no cell death to predict the growth inhibition resulting from cell cycle arrest only) to assess the respective contributions of cell cycle arrest and cell death to the overall growth inhibition induced by cytotoxic anticancer agents [18]. We used this cytostatic model to analyze the contribution of cell cycle arrest to overall growth inhibition when SNU-1 cells were treated with each cytotoxic agent. The time course of cell cycle distribution was determined in SNU-1 cells exposed to LOHP, 5-FU and PTX at IC_{80} levels, respectively, and used in model simulation (part of data shown in Fig. 3). Since the model uses the percentage of cells in each phase to simulate the growth of a cell population, predictions cannot be made with 0% in any phase at anytime. For this reason, this cytostatic model was used only for LOHP and PTX, but not for 5-FU, because in this case the percentage of cells in the G_2/M phase was zero after 12 h exposure (data not shown). The cytostatic computational model predicted 64% of the overall inhibition from the cell cycle arrest induced by LOHP after 72 h exposure at 7.55 μM. For PTX given for 72 h at 10 nM and 80% of the overall inhibition was attributed to cell cycle arrest by the model. These results indicate that the reduction in population growth rate caused by cell

Table 1 Parameters of the antiproliferative activities of LOHP, 5-FU, PTX and gefitinib against SNU-1 human gastric carcinoma cells

	LOHP	5-FU	PTX	Gefitinib
IC_{50}[a]	0.788 ± 0.142	9.35 ± 1.57	1.81 ± 0.67	13.2 ± 0.33
R[b]	5.00 ± 4.48	8.53 ± 7.64	32.0 ± 11.1	0
m[c]	0.811 ± 0.135	0.793 ± 0.125	5.02 ± 0.80	1.14 ± 0.10

Each value represents mean ± SD of three independent experiments.
[a] IC_{50} is the concentration of the drug that kills 50% of cancer cells compared to the control after 72 h of continuous exposure. Expressed in μM, except for paclitaxel, which is in nM.
[b] R is the residual unaffected fraction (resistance fraction) (1) and is equal to $(100 - E_{max})$.
[c] m is the Hill-type coefficient (1).

Fig. 3

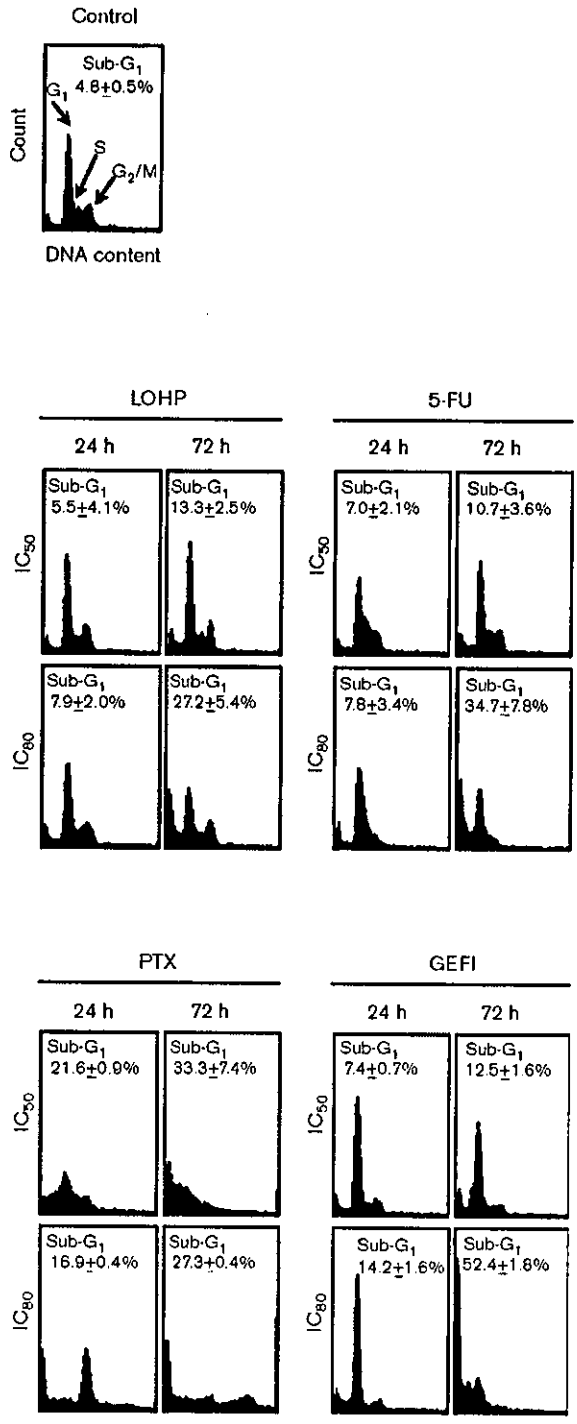

DNA histogram analysis in cells exposed to LOHP, 5-FU, PTX and gefitinib (GEFI) single treatment at IC_{50} and IC_{80}. Representative histograms are shown for 24 and 72 h post-treatment with the percentage of cells in sub-G_1 phase. Cells were harvested and fixed with ethanol before treated with RNase. Cells were then stained with propidium iodide and analyzed by flow cytometry. The concentrations were: 0.75 and 7.55 μM for LOHP, 9 and 65 μM for 5-FU, 2.5 and 10 nM for PTX, and 13 and 38 μM for GEFI.

additive. 5-FU + gefitinib was found additive with CI values ranging from 1.06 to 1.24. The combination of PTX + gefitinib showed greatest synergism: with CI values of less than 1.0 (0.28–0.99) for the whole f_a range; in particular, the resistant fraction associated with PTX single treatment was abrogated when combined with gefitinib, indicating a greater advantage compared to the other combinations (Fig. 4). For PTX + gefitinib, the most synergistic combination, the cell cycle arrest and apoptosis induction were studied in cells exposed to the simultaneous treatment of PTX and gefitinib at two different concentrations, i.e. 0.62 nM PTX + 4 μM gefitinib (combination IC_{50}) and 1.25 nM PTX + 8.5 μM gefitinib (combination IC_{65}) (Fig. 6). No significant changes in the cell cycle distribution were observed at the combination IC_{50} level until 72 h. At the higher concentration, i.e. 1.25 nM PTX + 8.5 μM gefitinib (around IC_{65}), a significant decrease in G_1 phase cells occurred with rapid increase in sub-G_1 cells. The simultaneous staining of DNA content and DNA strand breaks were used to discern the apoptotic cells as well as necrotic cells from viable cells (Fig. 6). The combination of PTX and gefitinib at the IC_{50} and IC_{65} level induced 100 and 35% increase ($p < 0.05$) in apoptosis (TUNEL-positive cells), respectively, compared to the single treatment, supporting the synergism between these two drugs.

Discussion

Systemic chemotherapy for the treatment of gastric carcinomas includes mitomycin C, anthracyclines, alkylating agents and 5-FU. Among these drugs, cisplatin and 5-FU are most commonly used in combination regimens. Recently, PTX has been added and a triplet combination of PTX, 5-FU and cisplatin has also been evaluated for the treatment of advanced gastric cancer [20]. In addition, a new platinum compound, LOHP, may replace cisplatin due to its reduced toxicity and decreased possibility of resistance development related to MMR deficiency. Hence, we undertook to evaluate in human gastric cancer cells the antitumor activities of LOHP, 5-FU and PTX, and the potential synergistic interactions between these cytotoxic agents individually and a newly developed target-based (cytostatic) drug, gefitinib, to provide preclinical data for the future clinical development of these agents in a combination setting for the treatment of advanced gastric carcinomas.

The *in vitro* antitumor activity of the four agents was evaluated by MTT assay. SNU-1 cells showed differential sensitivity toward these agents, and the rank order of sensitivities was PTX (1.81 nM) > LOHP (0.788 μM) > 5-FU (9.35 μM) > gefitinib (13.2 μM). Among these four agents, PTX showed the greatest cytotoxicity with an IC_{50} in the nanomolar range; however a significant

Fig. 4

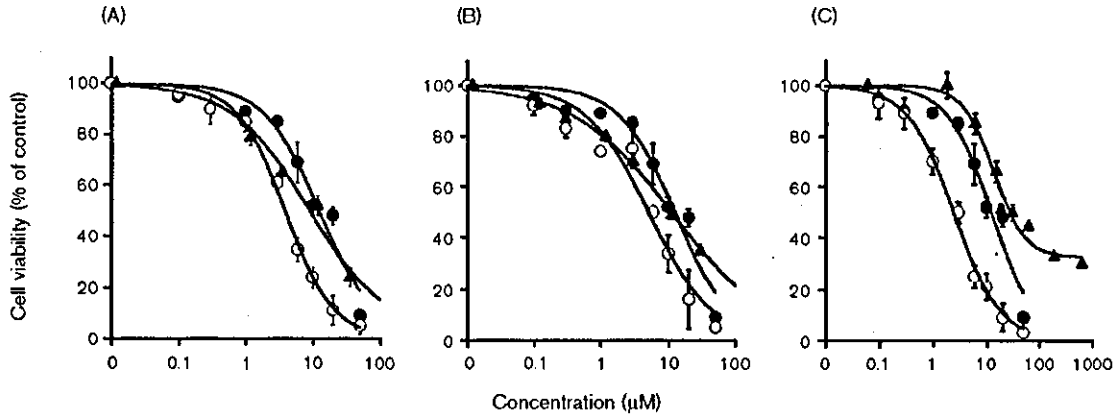

Representative dose–response curves of LOHP, 5-FU, PTX and gefitinib administered alone and in combination. (A) Gefitinib alone (solid circles), LOHP alone (solid triangles), LOHP + gefitinib (open circles); (B) gefitinib alone (solid circles), 5-FU alone (solid triangles), 5-FU + gefitinib (open circles); and (C) gefitinib alone (solid circles), PTX alone (solid triangles), PTX + gefitinib (open circles). Cells were simultaneously exposed to each treatment regimen for 72 h and cell viability was determined by MTT assay. The *x*-axis is [gefitinib] × 1, [LOHP] × 12, [5–FU] × 1.2 and [PTX] × 6250.

fraction of resistant cells was found (Table 1). Such PTX-resistant fractions have been observed in other cell lines, such as A549, a human lung adenocarcinoma cell line, and in FaDu, a pharynx squamous carcinoma cell line, when cell viability was measured by the MTT or the SRB assay (unpublished data). In the case of PTX, the growth-inhibitory effect as measured by two different methods produced different results, i.e. MTT versus direct cell counting (Table 1 and Fig. 2). The exposure of cells to 10 nM of PTX for 72 h induced around 90% growth inhibition, when determined by direct cell counting, whereas 68% growth inhibition was expected based on MTT data. In the cases of the other three agents, the MTT data agreed with direct cell counting. Therefore, the resistant fraction obtained in the MTT assay seemed to be associated with the assay method, especially for PTX, suggesting that the experimental data obtained by widely used viability assays, such as MTT and SRB, should be interpreted with caution when determining the cytotoxicity of PTX in monolayer cultures. However, in the present study, this did not affect the degree of synergy calculated for gefitinib + PTX since the maximum concentration of PTX used for the CI calculation was 2.5 nM, where no difference was observed between the cell counting and MTT results (Fig. 2).

Fig. 5

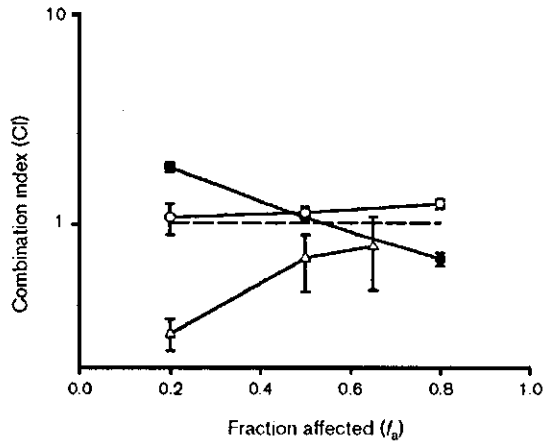

Combination index (CI_x) versus affected fraction (f_a) plots for LOHP + gefitinib (solid circles), 5-FU + gefitinib (open circles) and PTX + gefitinib (open squares) in SNU-1 cells. Cells were treated with LOHP or 5-FU or PTX + gefitinib at fixed equitoxic ratios. CI < 0.8, CI = 1 and CI > 1.2 indicate synergism, additivity and antagonism, respectively. LOHP and gefitinib were treated at a 0.083:1 molar ratio, 5-FU and gefitinib at 0.83:1, and PTX and gefitinib at 0.00016:1. CI_x was calculated using E_{max} model parameters obtained from the MTT data shown in Fig. 4.

SNU-1 cells showed significant resistance to 5-FU, i.e. the IC_{50} of 5-FU in SNU-1 cells was rather high (9.35 μM), which is close to that of gefitinib, a known cytostatic drug. MMR-proficient MKN-45 cells showed about 3 times higher sensitivity to 5-FU than SNU-1 cells (unpublished data). Hence, this intrinsic resistance of SNU-1 to 5-FU may be related to its MMR deficiency [15].

It has been suggested that the inhibition of EGFR-TK is an effective antiproliferative principle in EGFR-positive human gastric cancer cells [4]. Recently, gefitinib showed antiangiogenic and antiproliferative activity in a variety of human cancer cells *in vitro*, including human gastric cancer cells (KATO III and N87) [21]. The cytostatic growth inhibitory activity of gefitinib has been

Fig. 2

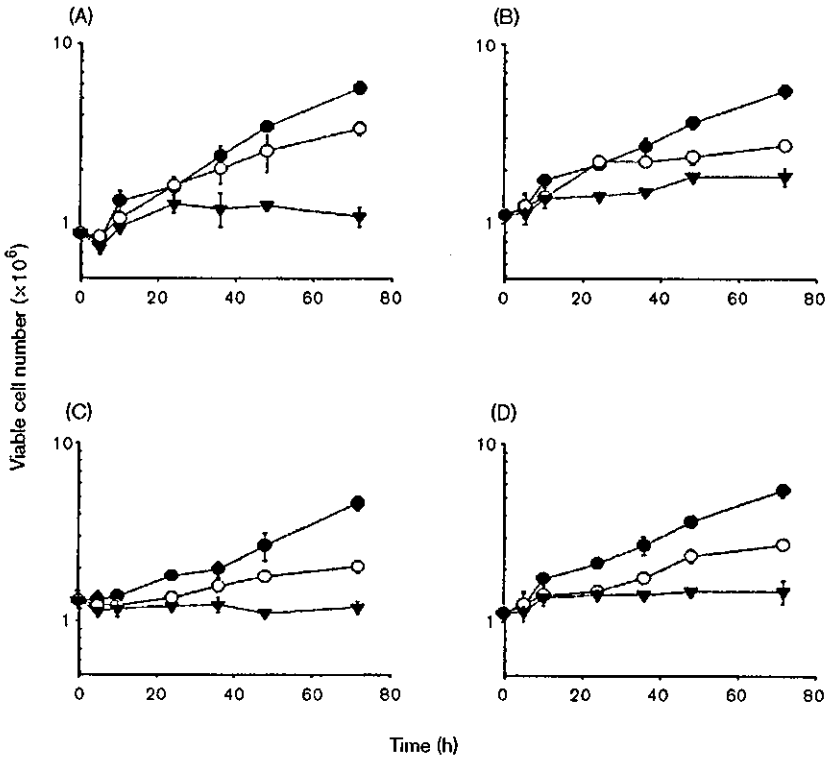

Growth curves of SNU-1 cells when incubated with (open circles, solid triangles) and without (solid circles) drug treatment: LOHP (A), 5-FU (B), PTX (C) and gefitinib (D). Cells were treated at two different concentrations near the IC_{50} (open circles) and the IC_{80} (solid triangles). The concentrations were: 0.75 and 7.55 μM for LOHP, 9 and 65 μM for 5-FU, 2.5 and 10 nM for PTX, and 13 and 38 μM for gefitinib. For cell number counting, cells were harvested by resuspending in medium and counted using a Coulter counter. Trypan blue exclusion was used for the determination of viable cell fraction.

cycle arrest effects contributes significantly to the overall growth inhibition induced by LOHP and PTX.

Cell cycle arrest effect with single drug treatment

The cell cycle arrest effect of the four agents was studied following a single drug exposure at two different concentrations for 72 h, i.e. around IC_{50} and IC_{80} as determined from the MTT dose–response curves. For LOHP, exposure to IC_{50} level concentrations, 0.75 μM did not induce significant changes in the cell cycle distribution (Fig. 3). When exposed to IC_{80} level concentrations, 7.55 μM of LOHP showed a moderate S phase decrease and G_2/M phase increase. Exposure to 5-FU (9 and 65 μM) resulted in an S phase increase along with G_2/M phase decreases in a concentration dependent manner: the cell cycle change following 5-FU treatment at the higher concentration (IC_{80}) was more pronounced. For LOHP and 5-FU, the sub-G_1 population, representative of cells that had undergone apoptosis, increased with time- and concentration-dependent manner. For PTX, cell cycle effect was dependent on drug concentration. At IC_{50} (2.5 nM), the number of cells in G_1 phase decreased with rapid accumulation of cells in sub-G_1 phase. At 10 nM, however, most cells were blocked in G_2/M phase (69.5 ± 0.8%) and a parallel decrease of the G_1 population was observed at 24 h, and a significant increase of the sub-G_1 population (27.4 ± 0.4%) and polyploid cells with ≥ 4*n* at 72 h. Gefitinib (13 and 38 μM) also showed a concentration dependent pattern of G_1 phase cell cycle arrest. The sub-G_1 population was induced after 72 h exposure at IC_{50} concentration (12.5 ± 1.6%) and increased to 52% after 72 h exposure at the concentration of 38 μM.

Evaluation of synergism

We evaluated the synergistic interaction between the cytotoxic agents, LOHP, 5-FU or PTX, and the cytostatic agent, gefitinib. All combinations were given at equitoxic ratios at the 50% inhibition levels of each drug, i.e. IC_{50} of drug A:IC_{50} of drug B. The dose–response curves are shown in Fig. 4 and the CI_x values calculated for $0.2 \leq f_a \leq 0.8$ (i.e. $20 \leq x \leq 80$) are shown in Fig. 5. CI_x values for the combination LOHP + gefitinib varied with f_a: CI_x decreased from 1.74 at $f_a = 0.2$ to 0.67 at $f_a = 0.8$. In the clinically relevant range of $f_a \geq 0.5$, hence, LOHP + gefitinib was considered to be synergistic to

Fig. 6

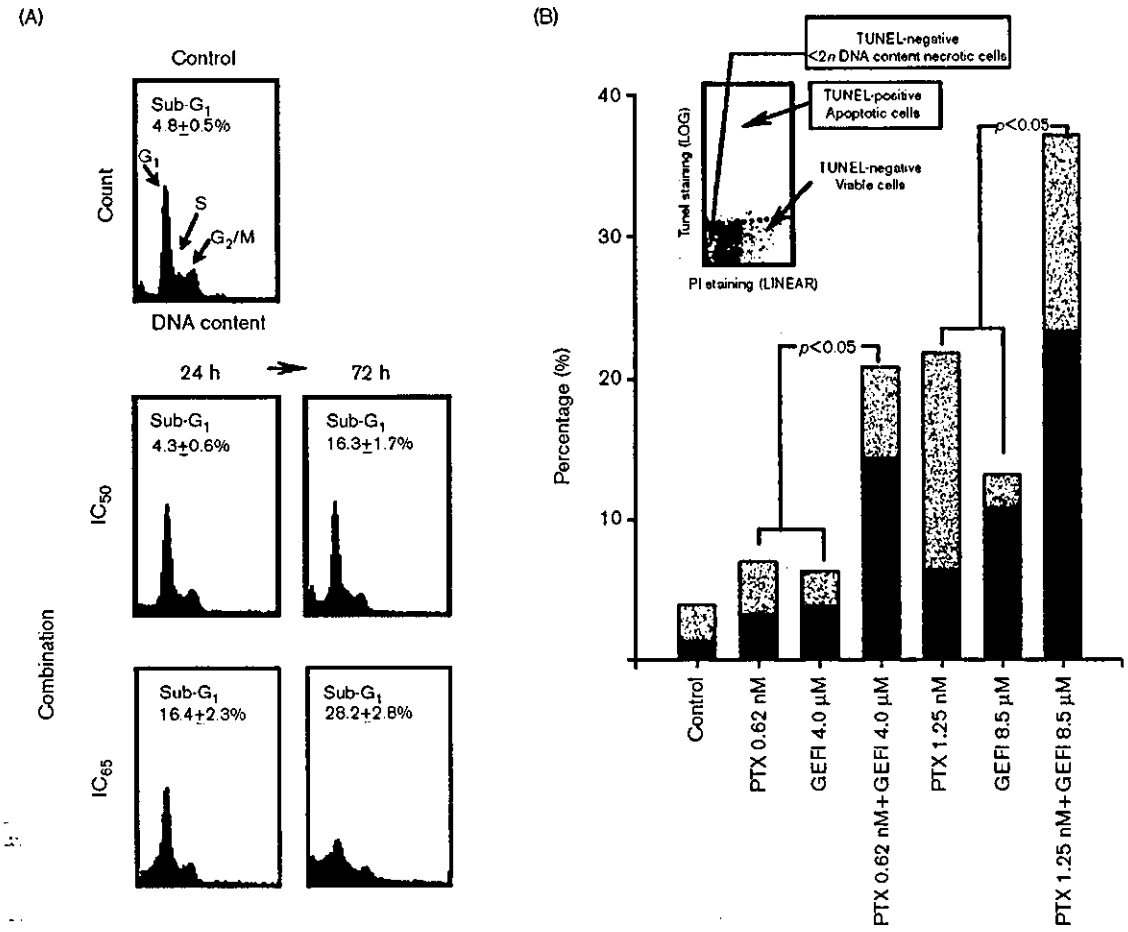

Cell cycle distribution and apoptosis induction during simultaneous treatment with PTX and gefitinib in SNU-1 cells. The drug concentrations used were 0.6 nM PTX + 4 μM (IC_{50}) or 1.25 nM PTX + 8.5 μM gefitinib (IC_{65}). (A) Representative histograms are shown for 24 and 72 h post-treatment with the percentage of cells in the sub-G_1 phase. At predetermined times following drug exposure, cells were harvested, fixed, stained with propidium iodide (PI) and analyzed by flow cytometry. (B) The bivariate analysis of DNA content and apoptosis in cells exposed to the indicated drug treatment for 72 h. Cells were treated for 72 h and processed for the double staining of TUNEL/PI and analyzed by flow cytometry. Solid box: TUNEL-negative necrotic cells; gray box: TUNEL-positive apoptotic cells. Statistical analysis: sum of PTX and gefitinib alone versus combination: $p < 0.05$.

demonstrated in a wide range of human cancer cell lines, and the reported IC_{50}s of gefitinib vary by cell line and by the assay method used. A soft agar colony assay showed an IC_{50} range of 0.05–2.5 μM for gefitinib in breast, colon and gastric cancer cells [8,21]. On the other hand, an IC_{50} range of 6–30 μM was reported in human head/neck and colon cancer cells by MTT [22,23]. Our results on the antitumor activity of gefitinib in SNU-1 cells are comparable with those obtained using the same viability assay method, i.e. MTT (Table 1).

A few studies have demonstrated an inverse correlation between growth IC_{50} and EGFR expression level [22], whereas contradictory data have been reported by others [7]. SNU-1 cells express moderate levels of EGFR, which may explain its moderate IC_{50} compared to other studies, which used highly overexpressing cell lines, such as A431. The EGFR signaling pathway involves the activation of several nuclear proteins, including cyclin D_1, via the activation of *ras* and mitogen-activated protein kinase [21]. Since EGFR activates cyclin D_1, and cyclin D_1 is required for cell cycle progression from G_1 to the S phase, EGFR signaling is critical for cell proliferation and its inhibition causes G_1 arrest in human cancer cells [21]. Our results also demonstrate that the inhibition of EGFR signaling by gefitinib induces G_1 arrest in human gastric cancer cells in a concentration dependent manner (Fig. 3).

In common with other cytostatic agents, gefitinib is expected to be a good candidate for combination regimens with cytotoxic agents. The combination of gefitinib + PTX has been shown to induce dose-depen-

dent cooperative growth inhibition and the potentiation of apoptosis *in vitro* [8,21], and to induce complete regression in some human tumor xenograft models [7]. Gefitinib + LOHP has been found to be supra-additive in human ovarian, breast and colon cells [14,24]. The sequence-dependent synergy appeared to be cell-line specific, i.e. gefitinib followed by cisplatin/5-FU was synergistic in head/neck cell cancer cell line [22], whereas gefitinib followed by oxaliplatin was antagonistic in human colon cancer cell line [25]. The simultaneous exposure was additive to synergistic in both studies, hence, the simultaneous schedule was to chosen to evaluate the synergy in the present study. We did not evaluate the sequence-dependent interactions because SNU-1 cells grow as a suspension and, hence, are not suitable for such experiments. The sequence dependency should be investigated using another human gastric cancer cell line.

In the present study, CI_* was calculated for the range of $0.2 \leq f_a \leq 0.8$ (Fig. 5), but the combination effect on cell cycle distribution and apoptosis induction was evaluated for the range of $f_a \geq 0.5$, i.e. at IC_{50} and IC_{80} levels (Fig. 6). Considering the fact that the maximum effect is needed in the clinical situation, it should be more relevant to focus on the effect above IC_{50} level [22]. Preclinical studies (especially, animal models) commonly use lower doses of chemotherapy to observe greater synergy; however, this often do not translate to the clinic, where maximum therapeutic doses are used [26].

In our study, the potentiation of antitumor activity was greatest for PTX + gefitinib, which had the lowest CI_{50} value among the three combinations and moreover the resistant fraction in the PTX single treatment was completely abrogated (Figs 4 and 5). LOHP + gefitinib is also a promising combination regimen because it produced a very similar level of synergism to PTX + gefitinib at $f_a = 0.8$ and additive effects at the $f_a = 0.5$ level. Gefitinib combined with PTX resulted in enhanced drug-induced apoptosis (Fig. 6). It is conceivable that the cytotoxicity of PTX is potentiated by the effective inhibition of survival signals upregulated by the EGFR signal network. The elucidation of the mechanism of this interaction requires further investigation.

Results of phase III lung trials for gefitinib + cytotoxics were disappointing and can be attributed to many factors including the following: (i) due to the lack of correlation between the apparent expression of EGFR and sensitivity, the responding phenotype was not known and patient selection could not be made, (ii) it is believed that triplet regimen of conventional chemotherapy are not superior to doublets in non-small cell lung cancer, and (iii) patients (in IDEAL phase II trials) who were already heavily treated with, and refractory to, chemotherapy may have been more sensitive to the inhibition of the EGFR pathway by gefitinib [27]. Despite the negative results of phase III lung trials, the rationales for studying the combination of gefitinib with cytotoxics in gastric cancers are 3-fold. (i) EGFR levels were associated with poor prognosis in gastric cancer patients [28,29], (ii) gefitinib is given orally, hence, higher drug concentration can be obtained in the gastric tissues and (iii) gastric cancers are relatively easy for biopsy study through which the responding phenotype can be identified.

In summary, the present study demonstrates that the antitumor activity of gefitinib, against human gastric carcinoma cells, is accompanied by significant cell cycle arrest and apoptosis. We also found that the antiproliferative effects of the cytotoxic drugs, LOHP and PTX, could be greatly enhanced when combined with gefitinib. The suppression of growth by gefitinib may be of clinical importance as the prolonged administration of orally active gefitinib could offer long-term control of gastric tumor growth and metastasis. This study provides preclinical data supporting the clinical development of gefitinib and its use in combination with PTX or LOHP against MMR-deficient human gastric cancers that express EGFR. Moreover, this study shows that gefitinib warrants further evaluation *vis-à-vis* its use in other gastric cancer cells/tumors.

References

1 Kim YH, Shin SW, Kim BS, Kim JH, Kim JG, Mok YJ, *et al.* Paclitaxel, 5-FU, and cisplatin combination chemotherapy for the treatment of advanced gastric carcinoma. *Cancer* 1999; 85:295–301.

2 Slesak B, Harlozinska A, Porebska I, Bojarowski T, Lapinska J, Rzeszutko M, *et al.* Expression of epidermal growth factor receptor family proteins (EGFR, c-erbB-2 and c-erbB-3) in gastric cancer and chronic gastritis. *Anticancer Res* 1998; 18:2727–2732.

3 Aoyagi K, Kohfuji K, Yano S, Murakami N, Miyagi M, Takeda J, *et al.* Evaluation of the epidermal growth factor receptor (EGFR) and c-erbB-2 in superspreading-type and penetrating-type gastric carcinoma. *Kurume Med J* 2001; 48:197–200.

4 Piontek M, Hengels KJ, Porschen R, Strohmeyer G. Antiproliferative effect of tyrosine kinase inhibitors in epidermal growth factor-stimulated growth of human gastric cancer cells. *Anticancer Res* 1993; 13:2119–2123.

5 Mendelsohn J, Fan Z. Epidermal growth factor receptor family and chemosensitization. *J Natl Cancer Inst* 1997; 89:341–343.

6 Caputo R, Tuccillo C, Manzo BA, Zarrilli R, Tortora G, Blanco Cdel V, *et al.* *Helicobacter pylori* VacA toxin up-regulates vascular endothelial growth factor expression in MKN 28 gastric cells through an epidermal growth factor receptor-, cyclooxygenase-2-dependent mechanism. *Clin Cancer Res* 2003; 9:2015–2021.

7 Sirotnak FM, Zakowski MF, Miller VA, Scher HI, Kris MG. Efficacy of cytotoxic agents against human tumor xenografts is markedly enhanced by coadministration of ZD1839 (Iressa), an inhibitor of EGFR tyrosine kinase. *Clin Cancer Res* 2000; 6:4885–4892.

8 Ciardiello F, Caputo R, Borriello G, Del Bufalo D, Biroccio A, Zupi G, *et al.* ZD1839 (IRESSA), an EGFR-selective tyrosine kinase inhibitor, enhances taxane activity in *bcl*-2 overexpressing, multidrug-resistant MCF-7 ADR human breast cancer cells. *Int J Cancer* 2002; 98:463–469.

9 Bevilacqua RA, Simpson AJ. Methylation of the hMLH1 promoter but no hMLH1 mutations in sporadic gastric carcinomas with high-level microsatellite instability. *Int J Cancer* 2000; 87: 200–203.

10 Kang YH, Bae SI, Kim WH. Comprehensive analysis of promoter methylation and altered expression of hMLH1 in gastric cancer cell lines with microsatellite instability. *J Cancer Res Clin Oncol* 2002; 128:119–124.

11 Fink D, Aebi S, Howell SB. The role of DNA mismatch repair in drug resistance. *Clin Cancer Res* 1998; 4:1–6.

12 Shin KH, Yang YM, Park J-G. Absence or decreased levels of the hMLH-1 protein in human carcinoma cell lines: implication of hMLH-1 in alkylation tolerance. *J Cancer Res Clin Oncol* 1998; 124:421–426.
13 Raymond E, Faivre S, Woynarowski JM, Chaney SG. Oxaliplatin: mechanism of action and antineoplastic activity. *Semin Oncol* 1998; 25:4–12.
14 Ciardiello F, Caputo R, Bianco R, Damiano V, Pomatico G, De Placido S, *et al.* Antitumor effect and potentiation of cytotoxic drugs activity in human cancer cells by ZD-1839 (Iressa), an epidermal growth factor receptor-selective tyrosine kinase inhibitor. *Clin Cancer Res* 2000; 6:2053–2063.
15 Carethers JM, Chauhan DP, Fink D, Nebel S, Bresalier RS, Howell SB, *et al.* Mismatch repair proficiency and *in vitro* response to 5-fluorouracil. *Gastroenterology* 1999; 117:123–131.
16 Carmichael J, Mitchell JB, DeGraff WG, Gamson J, Gazdar AF, Johnson BE, *et al.* Chemosensitivity testing of human lung cancer cell lines using the MTT assay. *Br J Cancer* 1988; 57:540–547.
17 Chou TC, Talalay P. Quantitative analysis of dose-effect relationships: the combined effects of multiple drugs or enzyme inhibitors. *Adv Enz Reg* 1984; 22:27–55.
18 Kuh HJ, Nakagawa S, Usuda J, Yamaoka K, Saijo N, Nishio K. A computational model for quantitative analysis of cell cycle arrest and its contribution to overall growth inhibition by anticancer agents. *Jpn J Cancer Res* 2000; 91:1303–1313.
19 Steel GG. *Growth Kinetics of Tumors: Cell Population Kinetics in Relation to the Growth and Treatment of Cancer.* Oxford: Clarendon Press; 1977.
20 Honecker F, Kollmannsberger C, Quietzsch D, Haag C, Schroeder M, Spott C, *et al.* Phase II study of weekly paclitaxel plus 24-h continuous infusion 5-FU, folinic acid and 3-weekly cisplatin for the treatment of patients with advanced gastric cancer. *Anticancer Drugs* 2002; 13:497–503.
21 Ciardiello F, Caputo R, Bianco R, Damiano V, Fontanini G, Cuccato S, *et al.* Inhibition of growth factor production and angiogenesis in human cancer cells by ZD1839 (Iressa), a selective epidermal growth factor receptor tyrosine kinase inhibitor. *Clin Cancer Res* 2001; 7: 1459–1465.
22 Magne N, Fischel JL, Dubreuil A, Formento P, Marcie S, Lagrange JL, *et al.* Sequence-dependent effects of ZD1839 ('Iressa') in combination with cytotoxic treatment in human head and neck cancer. *Br J Cancer* 2002; 86:819–827.
23 Magne N, Fischel JL, Dubreuil A, Formento P, Poupon MF, Laurent-Puig P, *et al.* Influence of epidermal growth factor receptor (EGFR), p53 and intrinsic MAP kinase pathway status of tumour cells on the antiproliferative effect of ZD1839 ('Iressa'). *Br J Cancer* 2002; 86:1518–1523.
24 Xu JM, Azzariti A, Colucci G, Paradiso A. The effect of gefitinib (Iressa, ZD1839) in combination with oxaliplatin is schedule-dependent in colon cancer cell lines. *Cancer Chemother Pharmacol* 2003; 52:442–448.
25 Xu JM, Azzariti A, Severino M, Lu B, Colucci G, Paradiso A. Characterization of sequence-dependent synergy between ZD1839 ('Iressa') and oxaliplatin. *Biochem Pharmacol* 2003; 66:551–563.
26 Herbst RS, Giaccone G, Schiller JH, Natale RB, Miller V, Manegold C, *et al.* Gefitinib in combination with paclitaxel and carboplatin in advanced non-small-cell lung cancer: a phase III trial—INTACT 2. *J Clin Oncol* 2004; 22:785–794.
27 Gamboa-Dominguez A, Dominguez-Fonseca C, Quintanilla-Martinez L, Reyes-Gutierrez E, Green D, Angeles-Angeles A, *et al.* Epidermal growth factor receptor expression correlates with poor survival in gastric adenocarcinoma from Mexican patients: a multivariate analysis using a standardized immunohistochemical detection system. *Mod Pathol* 2004; 17:579–587.
28 Kopp R, Rothbauer E, Ruge M, Arnholdt H, Spranger J, Muders M, *et al.* Clinical implications of the EGF receptor/ligand system for tumor progression and survival in gastrointestinal carcinomas: evidence for new therapeutic options. *Recent Results Cancer Res* 2003; 162:115–132.
29 Perez-Soler R. HER1/EGFR targeting: refining the strategy. *Oncologist* 2004; 9:58–67.

Translational research for lung cancer – An update

K. Nishio[1], S. Korfee[1,2], W. Eberhardt[2], N. Saijo[1], and T. Tamura[1]

[1]Shien-Lab, Medical Oncology, National Cancer Center Hospital and Pharmacology Division, National Cancer Center Research Institute, Tokyo, Japan.
[2]Department of Internal Medicine, West German Cancer Centre, Essen, Germany

Correlative studies at the National Cancer Center Hospital

Molecular correlative studies are essential for the development of anti-cancer molecular target drugs. One of the major purposes of a correlative study is "proof of principle" (POP). However, clinical POP studies for small molecules are usually more difficult to complete than POP studies for antibodies[1].

Since 2001, the National Cancer Center Hospital (Tokyo, Japan) has been operating as a laboratory for translational studies to develop molecular correlative studies. The laboratory members consist of medical oncologists, basic researchers, CRC research fellows, invited researchers from abroad, technicians, and statisticians. The laboratory is located next to the phase I wards in the hospital, enabling more than ten molecular correlative studies to be simultaneously performed. New clinical samples can be quickly obtained from patients (including outpatients), prepared for storage, and stored in the laboratory. The medical doctors working in the laboratory are often research fellows supported by government grants, since these individuals are often interested in this kind of research.

The location of the laboratory also gives medical oncologists the opportunity to frequently communicate with research members. The significance of study endpoints, study designs, technical and statistical information, and feasibility are frequently discussed, especially among young medical oncologists and researchers. As a result, young oncologists and researchers often collaborate in the proposal of new molecular correlative studies.

The major activities of the laboratory are pharmacokinetics or pharmacodynamics studies for early clinical studies (PI and PII) and reverse translational studies. Tissue banking and quality control are two of the most important activities. Part of the clinical sample testing is performed in collaboration with the CRO.

Gene expression profiles

Gene expression arrays (DNA chips) have already been used in clinical studies to predict response and in POP studies. Many kinds of DNA chips are now available. Oligonucleotide arrays containing more than 40,000 genes have recently become popular. These chips can be used differentially, depending upon the study's purpose. Before clinical use, however, an array's quality (linearity and reproducibility) should be determined in preclinical studies. At our center, the quality of each array is evaluated and expressed as the Pearson's product-moment coefficient of correlation. Based on the validated quality of the cDNA, protocols based on "experienced designs" are then established.

In clinical settings, sample quality and feasibility are often major limitations in the design of new studies. To maintain the quality of clinical samples, a system for sample flow has been established. First the purity of the nucleotides must be carefully examined. Purification methods largely depend on the tumor types. For example, brain tumors contain large amounts of carbohydrate chains, lung cancer samples are sometimes very hard, and breast cancer biopsy samples are lipid rich. These sample characteristics influence purification quality and efficiency.

After the gene expression profiles have been obtained for each samples, the data is analyzed using standardization, clustering, statistical analysis, and validation methods. Statistical and biological validation is essential. Ideally, clinical cross-validation studies should be performed for independent clinical studies. On the other hand, biomarkers can be validated in the same clinical study using the "leave-one out" method. The endpoint of these correlative studies is usually the selection of biomarkers for predicting response or toxicity. For such endpoints, the quality of the clinical study itself is also very important.

We have also used another endpoint in early clinical studies. We compared the clinical samples obtained before and after treatment. Analysis of gene alterations after treatment can be utilized for POP. We completed these correlative studies as part of clinical studies for multitarget tyrosine kinase inhibitors, farnesyl transferase inhibitor, and cytotoxic drugs.

For biological confirmation, we usually perform (semi-)quantitative RT-PCR or immunostaining. However, we recently discovered that "pathway analysis" is a powerful method for improving our understanding of the alteration of genes related to biological signal transduction

pathways. For the analysis of transcription factors, "network analysis" can be used to identify the signaling pathways of the transcription factors.

Correlative Study for TKI using New Array

We have several developed new arrays in collaboration with biocompanies as follows;.

Fiber Array To differentially identify the isotypes of target genes, such as beta-tubulin, we have developed a customized, highly quantitative "fiber array" for "antimitotic inhibitors". We will analyze the isotype-specific expression profile of beta-tubulin using this array.

Genotyping Array Recently, the EGFR mutation has become an exciting topic in research on tyrosine kinase inhibitors (TKI). Mutation analysis is now essential for any correlative studies for TKI. Patients with tumors containing the EGFR mutation in different exons are thought to have different responses to TKI[2, 3]. Whole exon (and intron) analysis can now be performed using the chip technology available in our laboratory. Additional mutations after treatment are also generating interest with regard to their role in acquired resistance to TKI.

Arrays for proteins Proteomics technology has been developed and successfully used to identify biomarkers for target-based drugs in a few clinical studies. Additional approaches, such as antibody arrays and "power blots", especially those using phospho-specific antibodies, should enable us to perform "kinome" analyses. Thus, these protein analysis technologies are now powerful tools for research on tyrosine kinase inhibitors.

References

1. Saijo N, Nishio K, Tamura T. Translational and clinical studies of target-based cancer therapy. *Int J Clin Oncol* 2003;8:187-92.0
2. Lynch TJ, Bell DW, Sordella R, Gurubhagavatula S, Okimoto RA, Brannigan BW, Harris PL, Haserlat SM, Supko JG, Haluska FG, Louis DN, Christiani DC, Settleman J, Haber DA. Activating mutations in the epidermal growth factor receptor underlying responsiveness of non-small-cell lung cancer to gefitinib. *N Engl J Med* 2004;350:2129-39.0
3. Paez JG, Janne PA, Lee JC, Tracy S, Greulich H, Gabriel S, Herman P, Kaye FJ, Lindeman N, Boggon TJ, Naoki K, Sasaki H, Fujii Y, Eck MJ, Sellers WR, Johnson BE, Meyerson M. EGFR mutations in lung cancer: correlation with clinical response to gefitinib therapy. *Science* 2004;304:1497-500.0

Int. J. Cancer: 108, 679–685 (2004)

Publication of the International Union Against Cancer

hnRNP L ENHANCES SENSITIVITY OF THE CELLS TO KW-2189

Fumiko TAGUCHI[1,3], Hitoshi KUSABA[1], Akira ASAI[4], Yasuo IWAMOTO[1], Keiichi YANO[4], Hirofumi NAKANO[4], Tamio MIZUKAMI[4], Nagahiro SAIJO[2], Harubumi KATO[3] and Kazuto NISHIO[1]*

[1]*Pharmacology Division, National Cancer Center Research Institute, Tokyo, Japan*
[2]*Medical Oncology Division, National Cancer Center Hospital, Tokyo, Japan*
[3]*Department of Surgery, Tokyo Medical University, Tokyo, Japan*
[4]*Tokyo Research Laboratories, Kyowa Hakko Kogyo Co. Ltd, Tokyo, Japan*

Heterogeneous nuclear ribonucleoproteins (hnRNPs) are involved in several RNA-related biological processes. We demonstrated hnRNP L as a candidate protein of DARP (duocarmycin-DNA adduct recognizing protein) by gel shift assay and amino acid sequencing. Stable transfectants of hnRNP L showed high sensitivity of the cells to the growth inhibitory effect of KW-2189, a duocarmycin derivative *in vitro*. Immunostaining of hnRNP L demonstrated differential intracellular localization of hnRNP L among human lung cancer cell lines. A transfection study using a series of deletion mutants of hnRNP L fused to indicated that the N-terminal portions of RRM(RNA recognition motif)1, RRM3 and RRM2 are involved in localization of hnRNP L. We identified sequences in these portions that have high homology with the sequences of known NLS (nuclear localization signal) and NES (nuclear export signal). hnRNP L is a factor that determines the sensitivities of cancer cells to the minor groove binder, and overexpression and differential intracellular localization of hnRNP L are involved in its function in lung cancer.

Key words: *hnRNP L; KW-2189; duocarmycin; minor groove binder; nuclear localization signal*

Heterogeneous nuclear ribonucleoproteins (hnRNPs) participate in a variety of processes involving RNA, including transcription, splicing, processing, translation and turnover, and there are approximately 20 major members of the hnRNP family.[1] High expression of some of these have been reported in several human malignant tumors and interest in the action of these proteins in malignancies has been growing.[2,3] HnRNP L is 68 kDa protein with 4 RNA recognition motifs (RRM). There have been several interesting reports demonstrating that cytoplasmic hnRNP L specifically interacts with VEGF mRNA in hypoxic cells *in vivo*, regulates VEGF mRNA stability[4] and binds in a sequence-specific manner to a *cis*-acting RNA sequence element that enables intron-independent gene expression.[5] The role of hnRNP L, however, still requires further study.

KW-2189 is a water-soluble derivative of antitumor antibiotic duocarmycin (DUM),[6–8] and DUM and its derivatives have been reported to exert their anti-tumor activity through covalent binding to the DNA minor groove and inhibition of DNA synthesis. We identified previously a nuclear protein DARP (duocarmycin-DNA adduct recognizing protein) in human cervical carcinoma HeLa S3 cells.[9] We purified the DARP from nuclear extract of HeLa S3 and its amino acid sequence was identical to hnRNP L. We investigated this, particularly in cancer cells.

MATERIAL AND METHODS

Cell cultures and reagents

Human small cell lung cancer cell lines SBC-3 and H69, human non-small cell lung cancer cell lines PC-14, and their respective cisplatin-resistant cell lines (SBC-3/CDDP, H69/CDDP,[10] and PC-14/CDDP[11]) were maintained in RPMI 1640 (Sigma, St. Louis, MO) supplemented with 10% heat-inactivated FBS (Gibco BRL, Gaithersburg, MD). Murine fibroblast cell line NIH3T3 and sublines (including cDNA transfectants) were cultured in DMEM (Nissui Pharmaceutical Co. Ltd., Tokyo, Japan) supplemented with 10% FBS. KW2189 was provided by Kyowa Hakko Kogyo Co., Ltd. A monoclonal antibody specific for hnRNP L (4D11) was generously provided by Dr. G. Dreyfuss (University of Pennsylvania, Philadelphia).

Cell extracts

Cells were washed twice with cold PBS and lysed in buffer (10 mM Tris-HCl pH 7.8, 1% Nonidet P-40, 0.15 M NaCl, 1 mM EDTA, 10 μg/ml aprotinin, 0.5 μg/ml leupeptin, 1 mM phenylmethane-sulfonyl fluoride [PMSF], 1 tablet/50 ml φgrComplete™ and 10% glycerol) for 60 min on ice. The lysates were centrifuged at 8,000*g* for 20 min, and supernatants were obtained as total protein. Protein concentration was measured by bicinchoninic acid protein assay (Pierce, Rockford, IL).

SBC-3, PC-14 and H69 cells were lysed in buffer A containing 10 mM HEPES-KOH (pH 7.9), 10 mM KCl, 0.1 mM EDTA-NaOH (pH 8.0), 0.1 mM ethyleneglycol bis(2-aminoethyl ether) tetraacetic acid (EGTA), 1 mM dithiothreitol (DTT), 0.5 mM PMSF, 1 mM aprotinin, and leupeptin. Nonidet P-40 (final concentration 0.5%) was added after allowing to stand on ice for 15 min. The supernatant obtained by centrifugation at 7,000*g* for 30 sec after standing on ice for 5 min was collected as the cytoplasmic fraction. The pellet was resuspended with buffer A containing 0.25 M sucrose, and after buffer B′ (buffer A containing 0.6 M sucrose) was added, the solution was centrifuged at 5,000*g* for 1 min at 4°C. The nuclei, which were contained in the pellet, were sonicated in buffer C containing 20 mM HEPES-KOH (pH 7.9), 0.4 M NaCl, 1 mM EDTA-NaOH (pH 8.0), 1 mM EGTA, 1 mM DTT and 1 mM PMSF, and then rocked at 4°C for 30 min and centrifuged at 8,000*g* for 10 min. The supernatant was used as the nuclear fraction. The nuclear protein content was adjusted to 5 μg per well, and the same volume of cytoplasmic protein was applied to the next well. The cytoplasmic and nuclear fractions were subjected to SDS-PAGE and Western blotting with anti-hnRNP L antibody.

Western blotting

An INSTA-Blot human tissues membrane (Imgenex, San Diego, CA), which contains 10 μg per lane of different human tissue lysates, was soaked in 100% methanol and then washed with TBST. After blocking the membrane in 5% skim milk in TBST for 1 hr at room temperature, it was probed with anti-hnRNP L antibody diluted (1:500) in TBST with 1% skim milk for 1 hr at

Fumiko Taguchi is a recipient of Research Resident Fellowship from the Foundation for Promotion of Cancer Research in Japan

*Correspondence to: Pharmacology Division, National Cancer Center Research Institute, 5-1-1 Tsukiji, Chuo-ku, Tokyo 104-0045, Japan. Fax: +81-3-3547-5185. E-mail: knishio@gan2.res.ncc.go.jp

Received 16 September 2002; Revised 25 August 2003; Accepted 12 September 2003

DOI 10.1002/ijc.11616

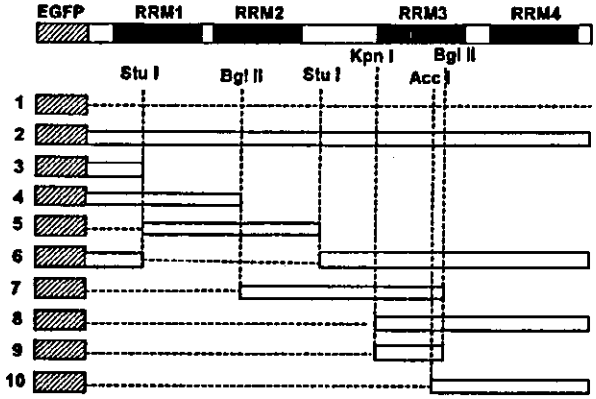

FIGURE 1 – Diagram of EGFP-hnRNP L deletion mutants. Known motifs, RNA recognition motifs (RRMs) 1, 2, 3 and 4 are boxed. The dark gray box denotes EGFP. Ten plasmids containing various parts of hnRNP L were constructed. The restriction sites used to generate deletion mutants are indicated.

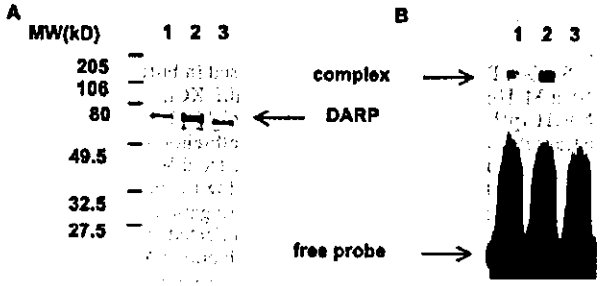

FIGURE 2 – Purification of DARP. (*a*) SDS-PAGE analysis of DEAE-sephacel fractions. *Lane 1*, 0.15 M KCl eluate; *Lane 2*, 0.2 M KCl eluate; *Lane 3*, 0.25 M KCl eluate. (*b*) Gel mobility shift assay of DEAE-sephacel fractions. *Lane 1*, 0.15 M KCl eluate; *Lane 2*, 0.2 M KCl eluate; *Lane 3*, 0.25 M KCl eluate. The oligonucleotides used as a probe contains the 5'-ATTA-3' sequence recognized by DUMSA (5'-GATC-CGGGATTACGATCGGGAGTCCCAGATTACGGCACCT-3'). The duplex oligonucleotides was incubated with each eluate after treatment with DUMSA as described in Material and Methods.

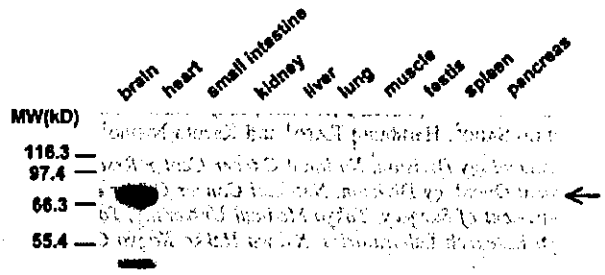

FIGURE 3 – Expression of hnRNP L in human tissues. Western blot analysis was carried out with anti-hnRNP L antibody. The membrane (INSTA-Blot) contains 10 μg per lane of different human tissue lysates. The arrow points to the hnRNP L protein.

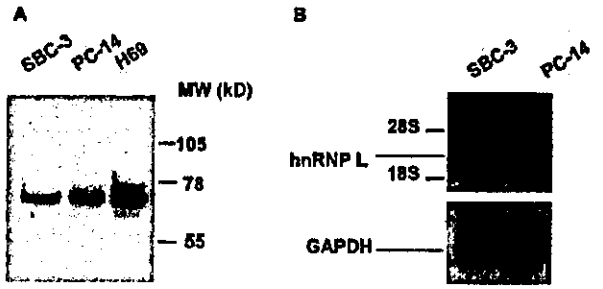

FIGURE 4 – Expression of hnRNP L in human lung cancer cell lines. (*a*) Cell lysates were prepared from 3 human lung cancer cell lines, separated with 7.5% SDS-PAGE, transferred to a membrane, and probed with anti-hnRNP L antibody. (*b*) Northern blotting was carried out with the 1030 bp fragment from hnRNP L cDNA as the probe.

room temperature, washed 3 times in TBST, incubated with anti-mouse IgG horseradish peroxidase antibody diluted (1:5000) in TBST with 1% skim milk for 1 hr at room temperature, and then washed 3 times in TBST. The signal was visualized with ECL (Amersham Pharmacia Biotech UK Ltd., Buckinghamshire, England), and Hyperfilm-MP (Amersham) was exposed to it.

Purification of DARP and amino acid sequencing

Purification of DARP was conducted as described previously.[9] DARP was detected by its ability to bind to DUMSA (one of DUMs)-DNA adduct in gel shift assays. Nuclear and cytoplasmic extracts from HeLa S3 cells (ATCC: American Type Culture Collection) were prepared according to previously published procedures. For identification of the DARP band, the aliquot of this material was subjected to DEAE-sephacel column again, and eluted with 0.5M stepwise procedure (0.1–0.5 M KCl) to give the small amount of purified DARP. Protein concentrations were estimated using Bio-Rad protein assay and the quality of the each fraction was checked by CBB (Coomassie brilliant blue) or silver staining of SDS-polyacrylamide gels. For analysis of amino acids sequence of DARP about 2 μg of affinity purified DARP was separated by 12% SDS-PAGE. The 60 kDa protein band was excised and digested with lysyl endopeptidase (WAKO, Japan) in 0.1 M Tris-HCl (pH 9.0), 4 M urea at 37°C for 16 hr. The resulting peptides were isolated by reversed phase HPLC on a RPC C2/C18 column (Amersham Pharmacia Biotech, Sweden). The amino acid sequence was determined by automated Edman degradation using a PPSQ-10 protein sequencer (Shimadzu, Japan).

Gel mobility shift assay

Labeled oligonucleotide (1 μg) was incubated with cell extract (final protein concentration, 20 μg/μl) at 30°C for 30 min in the presence of 2 μg of poly[dIdC]poly[dIdC] and 1 μg of BSA, except where stated, in a final volume of 15 μl of 0.1 M KCl HEDG. Where indicated, drug modified or unmodified calf thymus DNA was added to the reactions. Samples were electrophoresed in 6% polyacrylamide gel, dried and scanned.

Stable transfectants

Total RNA was prepared from HeLa cells with ISOGEN (Nippon Gene, Tokyo, Japan), and 14–784 and 636—1718 fragments of hnRNP L (2033 bp) were obtained by reverse transcription-polymerase chain reaction (RT-PCR). The PCR products were cloned in PCR II, a TA cloning plasmid vector, and then coupled at the Bcl I site. Subsequently, a fragment including hnRNP L was digested from the plasmid with Not I, and it was informed into the Not I site of the pRc/CMV vector. After confirming its sequence, this expression vector, pRc/CMV, containing cDNA of hnRNP L, was transfected into NIH3T3 cells with the Lipofectin reagent (Gibco BRL) according to the manufacturer's instructions. After 48 hr incubation, 1.5 mg/ml of G418 (Sigma) was added. Cells resistant to neomycin were selected, and isolated by limiting dilution methods.

Northern blotting

Total RNAs were prepared from SBC-3, PC-14 and NIH3T3 cells, and the 10 stable transfectants described above with ISO-